TÜBİTAK

Turkish Journal of Chemistry

http://journals.tubitak.gov.tr/chem/

Research Article

Turk J Chem
(2015) 39: 897 – 903
© TÜBİTAK
doi:10.3906/kim-1501-124

A comparative study on fabrication of Cu_2ZnSnS_4 (CZTS) nanofibers using acetate and chloride metal precursors

Burak Zafer BÜYÜKBEKAR[1,2], Faruk ÖZEL[3], Hüseyin ŞAKALAK[1,2], Halit ÇAVUŞOĞLU[1,2], Mustafa ERSÖZ[1,5], Mahmut KUŞ[1,4], Mustafa Selman YAVUZ[1,2,*]

[1]Advanced Technology Research and Application Center, Selçuk University, Konya, Turkey
[2]Department of Metallurgy and Materials Engineering, Selçuk University, Konya, Turkey
[3]Department of Materials Science and Engineering, Karamanoğlu Mehmetbey University, Karaman, Turkey
[4]Department of Chemical Engineering, Selçuk University, Konya, Turkey
[5]Department of Chemistry, Selçuk University, Konya, Turkey

Received: 28.01.2015 • **Accepted/Published Online:** 02.05.2015 • **Printed:** 28.08.2015

Abstract: This study reports, for the first time, the fabrication of electrospun Cu_2ZnSnS_4 (CZTS) nanofibers using metal acetate precursors. Viscous poly(vinyl pyrrolidone) (PVP) solution containing acetate or chloride salts of copper, zinc, and tin was electrospun onto a conductive substrate. The PVP nanofibers that have a mixture of metal salts were annealed at elevated temperatures. After calcination, these nanofibers were treated with the sulfur source and then annealed again in order to generate CZTS nanofibers. The CZTS nanofibers generated from acetate and chloride salts were characterized and compared. Belt-like and wire-like nanofibers were obtained when using metal acetate and chloride precursors, respectively.

Key words: Electrospinning, nanofibers, kesterite, solar energy materials, polymers

1. Introduction

Chalcogenide-based solar cells have received great attention due to their low cost and high efficiency in comparison with the commercial photovoltaic (PV) technologies.[1] In particular, indium-free quaternary chalcogenides (Cu_2ZnSnS_4 (CZTS), $Cu_2ZnSnSe_4$ (CZTSe)) are promising materials for their potential applications in solar cells due to their high absorption efficiency, direct band gap around 1.0–1.5 eV, and low toxicity.[2] CZTS or CZTSe materials have two basic crystal structures known as stannite and kesterite types.[3] These structures are similar, but have different arrangements of Cu and Zn atoms. Kesterite phase is mostly dominant because of its better stability to the stannite ones.[4] CZTS, a p-type semiconductor, has been generally used in p-n junction solar cells as an n-type semiconductor like CdS.[5–8] CZTS films have also been used as counter electrode in dye sensitized solar cells.[9] There have been many reports on solution-based synthesis of kesterite and stannite CZTS materials including nanocrystals, nanowires, and nanosheets.[10] However, the complicated procedures and the production of extra toxic byproducts are often the main obstacles in these solution-based syntheses. On the other hand, a simple and popular method, electrospinning, could be applied to fabricate CZTS fibers with a greater advantage of large-scale production capability.

Nanofibers have been used in many applications such as membranes, filtration, protective masks, drug

*Correspondence: selmanyavuz@gmail.com

delivery, biosensing, pharmaceuticals, and tissue engineering due to their light weight, possession of large surface areas, various functionality, and high mechanical strength.[11–14] To fabricate nanofibers, electrospinning is the most common and easy technique to prepare. The chemical composition of the fibers and the fiber diameter can easily be controlled depending on the operating parameters, chemical composition, and physical properties of the solution.[15–21] Over the last decade, the synthesis of ceramic nanofibers and nanowires using electrospinning has been widely used. In these syntheses, electrospinnable polymers such as polyvinyl pyrrolidone (PVP), polyvinyl alcohol (PVA), and cellulose acetate were used as a sacrificial nanofiber template. Upon calcination of a polymeric nanofiber containing metal precursors, the decompositions of these precursors generate the metallic nanostructures without changing nanofiber form. We had previously fabricated TiO_2 and ZrO_2 nanofiber membranes after calcinations of sacrificial PVP nanofibers containing titanium and zirconium salts.[12] This technique was applied to fabricate a variety of metal nanofibers. There have been a very limited number of reports on the fabrication of CZTS nanofibers to date.[22–25] In these CZTS nanofibers, only chloride salts have been used.

In the present study, we fabricated, for the first time, electrospun CZTS nanofibers through using a metal precursor that has acetate salts. PVP solution containing copper, zinc, and tin salts was used for electrospinning onto the conductive substrate. The PVP nanofibers that have a mixture of metal salts were annealed at various conditions. In addition to wire structure, belt-like structures were observed depending on the reaction conditions. The metal nanofibers generated from acetate and chloride salts were also compared.

2. Results and discussion

We fabricated Cu_2ZnSnS_4 (CZTS) nanofibers using a modified protocol that was mainly electrospinning a polymer solution containing sol-gel precursors.[12] We first electrospun the polymer-metal salt mixture onto a simple aluminum foil, grounded electrode, and then calcinated it in the presence of sulfur source to produce the metallic CZTS nanofibers. Figure 1 shows the SEM micrographs of Cu_2ZnSnS_4 (CZTS) fibers during each fabrication step. The optimum parameters for the best fiber morphology were obtained when acetate salts were used as precursors with a molar ratio of 4:4:2 for Cu, Zn, and Sn, respectively. As is clear from Figure 1, the structure of fibers strongly depends on the electrospinning parameters. Figures 1a and 1b show a nonwoven mat, PVP nanofibers, which have metal acetate salts. Using acetate salts of metals as the precursors, belt-like structures were obtained as shown in Figures 1a and 1b. Before thermal annealing, belt-like surfaces were observed to be almost smooth. This was an expected observation, because fibers were not crystalline yet and still contained PVP (Figures 1a and 1b). After annealing at 500 °C for 1 h, the composite nanobelts were converted into crystalline nanofibers. As shown in Figures 1c and 1d, the crystalline fibers had a diameter of roughly 250–300 nm with irregular rough surfaces having small beads. The beads were most probably formed due to aggregation of metal salts on contact points. Figures 1e and 1f show a second thermal annealing of metal nanofibers with dodecanethiol in order to produce CZTS nanofibers. The belt-shaped CZTS nanofibers remain irregular wires after the second annealing.

Figure 2 shows SEM images of CZTS fibers fabricated with a mixture of PVP and chloride metal salts. It is clear from Figure 2 that, compared to the CZTS nanofibers generated from metal acetate salts, the morphology of the nanofibers was converted to wire-like nanofibers by using metal chloride salts. Figures 2a and 2b show the PVP nanofibers that have metal salts before annealing. Wire-like fibers with a very smooth surface morphology are clearly observed. Thermal annealing at elevated temperature leads to the removal of PVP and crystallization of CZTS structures (Figures 2c and 2d). During crystallization, the smooth surface

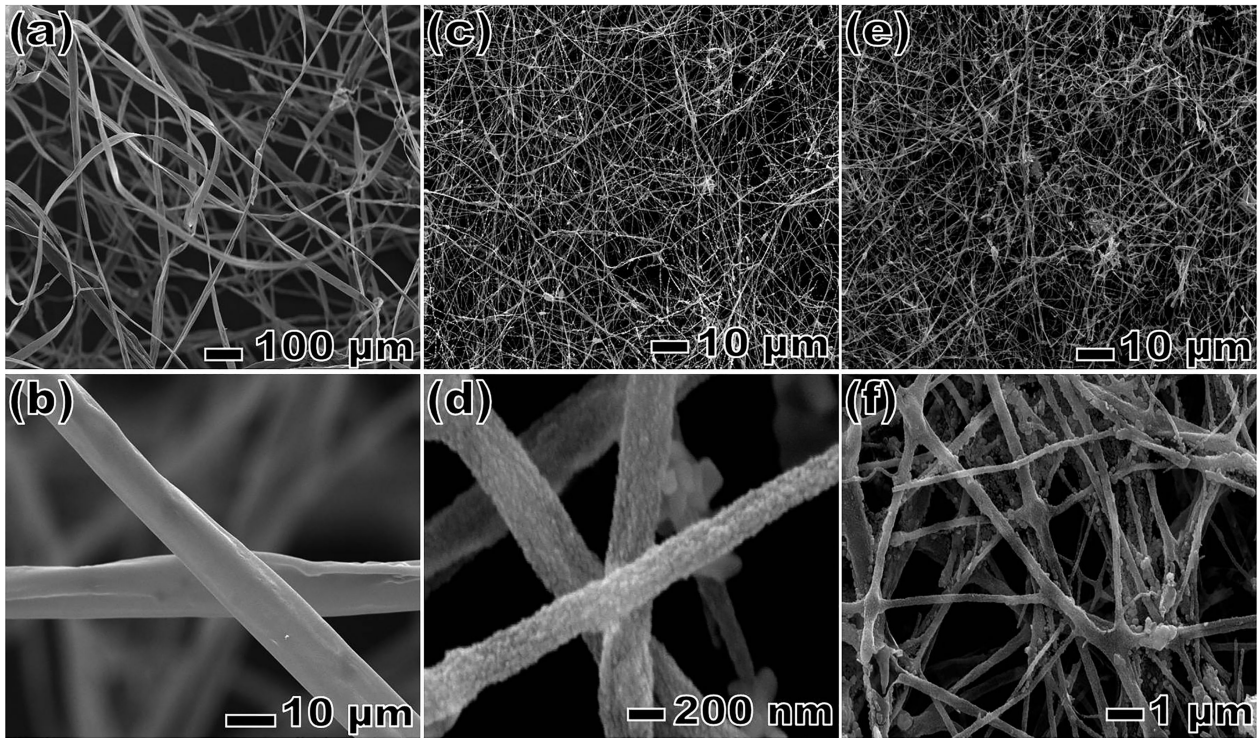


Figure 1. SEM images of CZTS fibers that use acetate precursors. PVP fibers that contain metal acetate salts (a, b), after annealing without dodecanethiol (c, d), and then after second annealing with dodecanethiol (e, f).

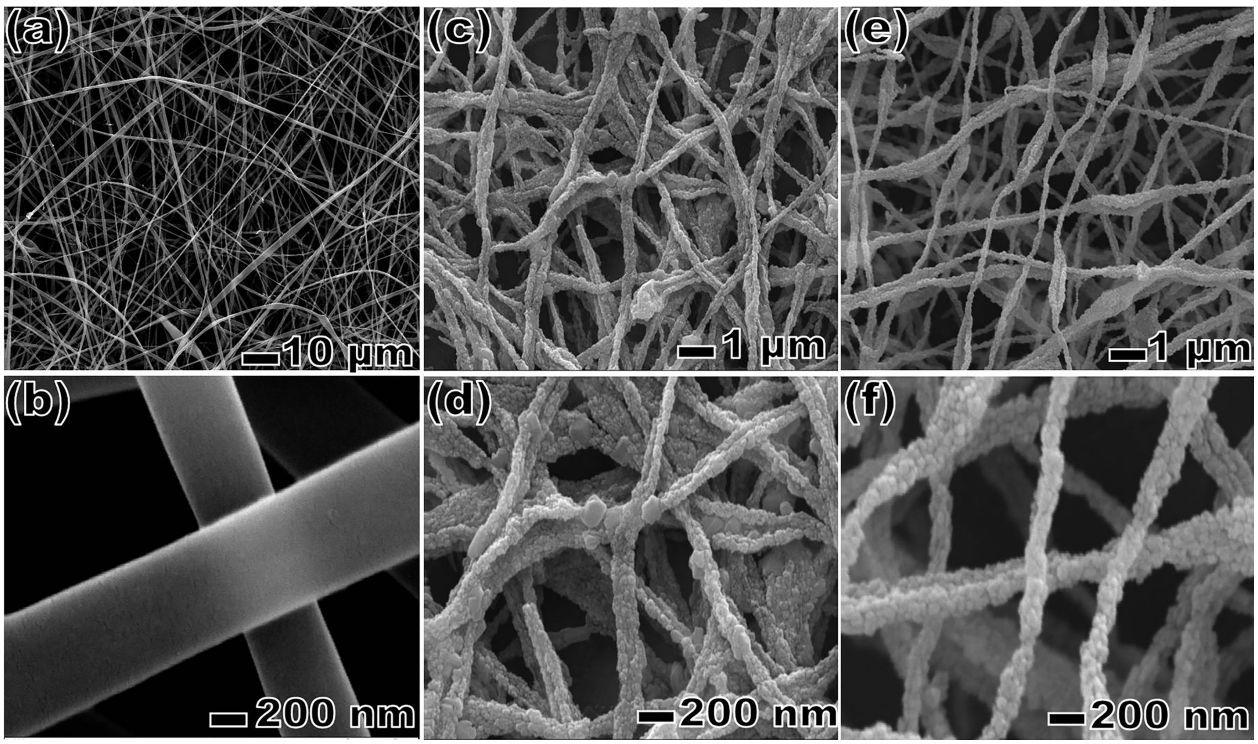


Figure 2. SEM images of CZTS fibers that use chloride precursors. PVP fibers that contain metal chloride salts (a, b), after annealing without dodecanethiol (c, d), and then after second annealing with dodecanethiol (e, f).

morphology of nanofibers was converted to rough and wire-like nanofibers with smaller sizes. The average size of the CZTS nanofibers decreased from 400 nm to 150 nm after thermal annealing. Alkyl thiols, the sulfur source, were drop cast onto these nanofibers and then annealed at elevated temperature for the second time in order to fabricate CZTS nanofibers as shown in Figures 2e and 2f. It can be noted that the CZTS nanofiber morphology remains in similar fiber morphology as in Figures 2c and 2d. As a result, when the metal chloride salts were used as the metal precursors, a better fiber morphology and uniformity were obtained as compared to acetate ones.

Figure 3 shows typical transmission electron microscopy (TEM) images of CZTS nanofibers. The nanofibers obtained by using metal acetate precursors are shown in Figure 3a. Belt-like fibers with irregular-shape beads on the sides are clearly seen. On the other hand, in Figure 3b, the CZTS nanofibers generated by using metal chloride precursors have a wire-like morphology with irregular surfaces. In conclusion, both metal precursors end up as kesterite CZTS nanofibers but they have different morphologies (belt-like and wire-like).

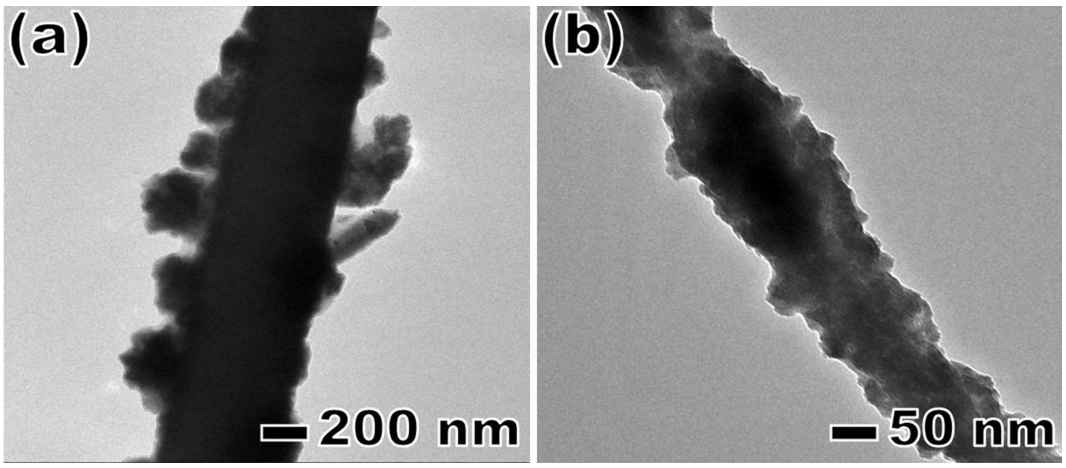


Figure 3. TEM images of CZTS fibers fabricated with acetate precursors (a) and with chloride precursors (b).

The absorption spectra of crystalline fibers are shown in Figure 4a. The band gap of the CZTS fibers is estimated to be 1.5 eV, which is in agreement with previous reports.[15,16] No structural or regional bands are observed, but a broad band with a long tail covers all the visible region.

Figure 4b shows X-ray diffraction (XRD) patterns of the nanofibers before and after the annealing process. The fabricated nanofibers obtained from both chloride and acetate precursors give very similar XRD patterns. As is clear from Figure 4b, the fibers before the annealing process show an amorphous phase while crystallization occurs after annealing. The peak shapes and diffraction angles confirm that the fabricated CZTS fibers show the kesterite crystal structure. Characteristic peaks corresponding to the planes of (112), (200), (220), (312), (008), (332) are clearly seen. All these diffraction planes are also in good agreement with JCPDS 26-0575. EDX results (not shown) also confirm that the structure consists of copper, zinc, tin, and sulfur in a ratio of 12:8:9:4, respectively.

3. Experimental

3.1. Materials

Copper (II) chloride dihydrate ($CuCl_2.2H_2O$), zinc chloride ($ZnCl_2$), tin(II) chloride dihydrate ($SnCl_2.2H_20$), and copper(II) acetate monohydrate $(CH_3COO)_2Cu.H_2O$ were obtained from Merck (Germany); 1-Dodechanethiol

(98%) and tin(II) acetate ($Sn(OOCCH_3)_2$) were obtained from ABCR and Alfa Aesar, respectively. Zinc acetate dihydrate ($C_4H_6O_4Zn.2H_2O$) and poly(vinyl pyrrolidone) (PVP, Mw = 1.3 × 10^6) were provided by Sigma-Aldrich. All chemicals were used as received. Deionized water was used as a solvent.

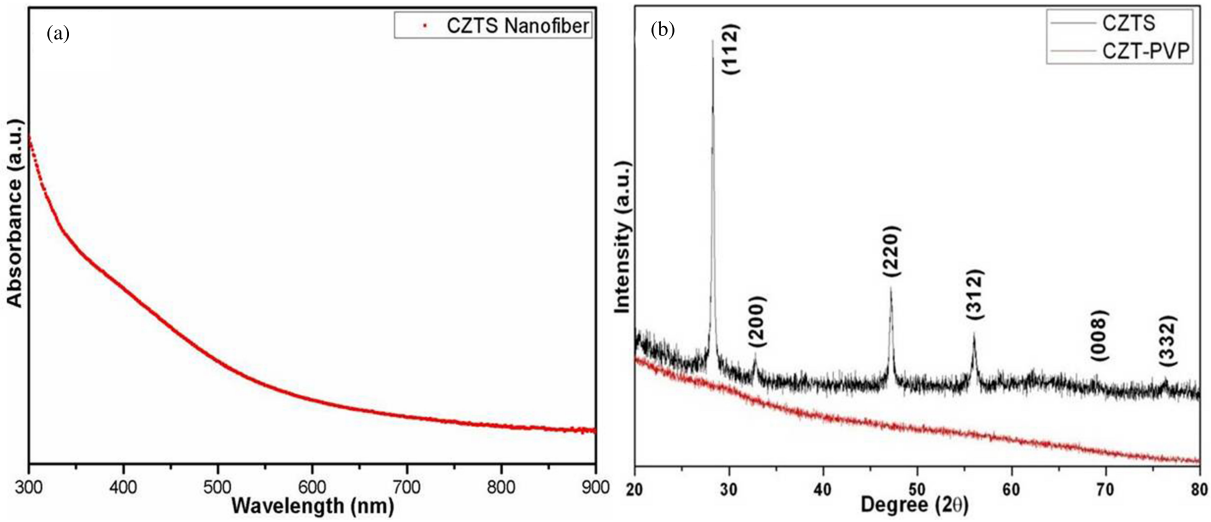


Figure 4. UV-Vis-NIR absorption spectrum of CZTS nanofibers (a), XRD pattern of CZTS fibers (b).

3.2. Instrumentation

Electrospinning was done using a Spellman SL30 brand DC power supply. A KD Scientific brand syringe pump was used. The XRD pattern of colloidal nanoparticles was recorded with a Bruker Advance D8 XRD (Cu α source with 1.5406 wavelength), in powder mode. A Zeiss Evo model scanning electron microscope (SEM) and JEOL JEM-2100F 200kV model transmission electron microscope were used to obtain SEM- EDX and TEM images, respectively. The optical properties of the as-prepared CZTS fibers were characterized by UV-Vis absorption spectroscopy (UV-Vis) recorded on a Biochrom Libra S22 UV-Vis spectrometer.

3.3. Fabrication of CZTS fibers through using acetate precursors

Fabrication of the CZTS fibers was typically achieved by electrospinning a solution containing 4 mmol (0.342 g) copper acetate, 2 mmol (0.136 g) of zinc acetate, 2 mmol (0.226 g) of tin(II) acetate, and 4 mL of deionized water. The mixture was mixed and stirred by homogenizer for 20 min. Then 0.5 g of PVP (Mw = 1.3 × 10^6) was added to the aqueous solution and the final mixture was stirred for 3 h. The solution was passed through a syringe with a 22 gauge stainless steel needle at the tip. The needle was electrified using a high-voltage DC supply (Spellman SL30) with an applied voltage of 20 kV. The solution was pumped continuously using a syringe pump (KD Scientific) at a rate of 2 mL/h. Fibers were collected on aluminum foil placed at a 15 cm vertical distance to the needle tip. Fibers were accumulated onto a grounded collector (typically, a piece of aluminum foil) and left overnight in air. The fibers were peeled off from the aluminum foil and placed in a crucible. The crucible was placed into a preheated oven at 500 °C for 3 h. The calcinated CZTS nanofibers were characterized using SEM, XRD, and UV-Vis. To generate the crystal CZTS fibers, dodecanethiol solution (2 mL) was added dropwise onto the CZT-PVP fibers and then the fibers were calcinated again in the oven at 500 °C for 3 h. Then the CZTS fibers were left to cool down at room temperature and characterized by using SEM, TEM, UV-Vis, and XRD.

3.4. Fabrication of CZTS fibers using chloride precursors

The procedure in which CZTS fibers were fabricated using acetate precursors was applied for the fabrication of CZTS fibers using chloride precursors. In this process, chloride salts were used instead of acetate ones. Mole ratios were kept constant.

4. Conclusion

We successfully demonstrated the fabrication of kesterite CZTS crystalline fibers using metal acetate and chloride precursors. The structure and morphology of the nanofibers strongly depend on the solution components. PVP solution that has copper, zinc, and tin salts was electrospun onto the conductive substrate and then annealed at elevated temperature. After introduction of dodecanethiol (sulfur source), the fibers were annealed again in order to fabricate CZTS nanofibers. The CZTS nanofibers were characterized using UV-Vis, SEM, TEM, and XRD. If metal acetate salts had been used, belt-like nanofibers would have been obtained. On the other hand, the wire-like nanofibers were observed when metal chloride salts were used. We think that these Cu_2ZnSnS_4 nanofibers are promising materials for photovoltaic and solar cell technology.

Acknowledgments

This study was carried out as a master thesis by Burak Zafer Büyükbekar at the Graduate School of Natural and Applied Science at Selçuk University, Konya, Turkey. This study was also supported by the Research Foundation of Selçuk University (BAP) and TÜBİTAK (Project No. 112M096, COST TD1004).

References

1. Todorow, T. K.; Reuter, K. B.; Mitzi, D. B. *Adv. Mater.* **2010**, *22*, 156–159.
2. Wang, J. J.; Hu, J. S.; Guo, Y. G.; Wan, L. J. *NPG Asia Materials* **2012**, *4*, 1–6.
3. Wang, H. *Int. J. Photoenergy* **2011**, *1*, 1–10.
4. Schorr, S. *Thin Solid Films* **2007**, *15*, 5985–5991.
5. Todorov, T. K.; Tang, J.; Bag, S.; Gunawan, O.; Gokmen, T.; Zhu, Y.; Mitzi, D. B. *Adv. Energy Mater.* **2013**, *3*, 34–38.
6. Fairbrother, A.; Hemme, E. G.; Roca, V. I.; Fontane, X.; Agudelo, F. A. P.; Galan, O. V.; Rodríguez, A. P.; Saucedo, E. *J. Am. Chem. Soc.* **2012,** *134*, 8018–8021.
7. Pawar, S. M.; Pawar, B. S.; Moholkar, A. V.; Choi, D. S.; Yun, J. H.; Moon, J. H.; Kolekar, S. S.; Kim, J. H. *Electrochim. Acta* **2010**, *55*, 4057–4061.
8. Scragg, J. J.; Berg, D. M.; Dale, P. J. *J. Electroanal. Chem.* **2010**, *646*, 52–59.
9. Xin, X.; He, M.; Han, W.; Jung, J.; Lin, Z. *Angew. Chem. Int. Edit.* **2011**, *50*, 11739–11742.
10. Ming, W.; Du, Q. Y.; Wang, D. C.; Liu, W. F.; Jiang, G. S.; Zhu, C. F. *Mater. Lett.* **2012**, *79*, 177–179.
11. Jiang, X.; Xie, Y.; Lu, J.; Zhu, L. Y.; He, W.; Qian, Y. T. *Chem. Mater.* **2001**, *13*, 1213–1217.
12. Formo, E.; Yavuz, M. S.; Lee, E. P.; Lane, L.; Xia, Y. *J. Mater. Chem.* **2009**, *19*, 3878–3882.
13. Lin, D.; Wu, H.; Zhang, R.; Pan, W. *J. Am. Ceram. Soc.* **2007**, *90*, 3664–3666.
14. Gu, S. Y.; Ren, J.; Vancso, G. J. *Eur. Polym. J.* **2005**, *41*, 2559–2568.
15. Li, D.; Xia, Y. *Nano Lett.* **2004**, *4*, 933–938.
16. Ding, Y.; Wu, Q.; Zhao, D.; Ye, W.; Hanif, M.; Hou, H. *Eur. Polym. J.* **2013**, *49*, 2567–2571.
17. Schueren, L. V.; Schoenmaker, B. D.; Kalaoglu, Ö. I.; Clerck, K. D. *Eur. Polym. J.* **2011**, *47*, 1256–1263.

18. Lingaiah, S.; Shivakumar, K. *Eur. Polym. J.* **2013**, *49*, 2101–2108.
19. Li, D.; McCann, J. T.; Xia Y.; Marquez, M. *J. Am. Ceram. Soc.* **2006**, *89*, 1861–1864.
20. Meng, F.; Zhan, Y.; Lei, Y.; Zhao R.; Xu M.; Liu, X. *Eur. Polym. J.* **2011**, *47*, 1563–1568.
21. Hsu, K. C.; Liao, J. D.; Yang, J. R.; Fu, Y. S. *Cryst. Eng. Comm.* **2013**, *15*, 4303–4308.
22. Chen, L. J.; Chuang, Y. J. *J. Power Sources* **2013**, *241*, 259–265.
23. Giray, D.; Balkan, T.; Dietzel, B.; Sarac, A. S. *Eur. Polym. J.* **2013**, *49*, 2645–2653.
24. Li, D.; Xia, Y. *Adv. Mater.* **2004**, *16*, 1151–1170.
25. Cozza, E. S.; Ma, Q.; Monticelli, O.; Cebe, P. *Eur. Polym. J.* **2013**, *49*, 33–40.